Separation Science and Technology
Publication details, including instructions for authors and subscription information:
http://www.informaworld.com/smpp/title~content=t713708471

Sorption of Carbon Dioxide onto Sodium Carbonate

Sang-Wook Park[a]; Deok-Ho Sung[a]; Byoung-Sik Choi[a]; Kwang-Joong Oh[a]; Kil-Ho Moon[b]
[a] Division of Chemical Engineering, Pusan National University, Busan, Korea [b] Doosan Heavy Industries & Construction Com. Ltd. R&D Center, Changwon, Korea

To cite this Article Park, Sang-Wook , Sung, Deok-Ho , Choi, Byoung-Sik , Oh, Kwang-Joong and Moon, Kil-Ho(2006) 'Sorption of Carbon Dioxide onto Sodium Carbonate', Separation Science and Technology, 41: 12, 2665 — 2684
To link to this Article: DOI: 10.1080/01496390600826659
URL: http://dx.doi.org/10.1080/01496390600826659

Separation Science and Technology, 41: 2665–2684, 2006

ISSN 0149-6395 print/1520-5754 online
DOI: 10.1080/01496390600826659

Sorption of Carbon Dioxide onto Sodium Carbonate

Sang-Wook Park, Deok-Ho Sung, Byoung-Sik Choi, and Kwang-Joong Oh
Division of Chemical Engineering, Pusan National University, Busan, Korea

Kil-Ho Moon
Doosan Heavy Industries & Construction Com. Ltd. R&D Center, Changwon, Korea

Abstract: Sodium carbonate was used as a sorbent to capture CO_2 from a gaseous stream of carbon dioxide, nitrogen, and moisture. The breakthrough data of CO_2 were measured in a fixed bed to observe the reaction kinetics of CO_2-carbonate reaction. Several models such as the shrinking-core model, the homogeneous model, and the deactivation model in the non-catalytic heterogeneous reaction systems were used to explain the kinetics of reaction among CO_2, Na_2CO_3, and moisture using analysis of the experimental breakthrough data. Good agreement of the deactivation model was obtained with the experimental breakthrough data. The sorption rate constant and the deactivation rate constant were evaluated by analysis of the experimental breakthrough data using a nonlinear least squares technique and described as Arrhenius form.

Keywords: Carbon dioxide, carbonates, breakthrough curve, deactivation model

INTRODUCTION

Carbon dioxide is the major atmospheric contaminant leading to temperature increase caused by the greenhouse effect. From 1750 until 1998 the

Received 25 January 2006, Accepted 10 April 2006
Address correspondence to Sang-Wook Park, Division of Chemical Engineering, Pusan National University, Busan 609-735, Korea. E-mail: swpark@pusan.ac.kr

concentration of CO_2 in the atmosphere has increased from 280 ppm to almost 380 ppm (1). Known anthropogenic sources account for 7 billion metric tons per year. The principal anthropogenic source is the combustion of fossil fuels, which accounts for about three-quarters of the total anthropogenic emissions of carbon worldwide (1). CO_2 emissions will correspondingly increase in the absence of any capture/sequestration strategy. In view that CO_2 is a greenhouse gas with the potential to contribute to global climate warming, existing and improved technologies to mitigate the release of CO_2 to the environment are being considered as a prudent precaution against global warming.

Carbon dioxide can be removed from flue gas and waste gas streams produced from carbon usage by various methods; absorption with a solvent, membrane separation, cryogenic fractionation, and adsorption using molecular sieves. Particularly, absorption has been widely used in the chemical industries by the Benfield Process (2). The capture of CO_2 from each of these processes is costly (1). Another technique for removal of CO_2 is dry scrubbing or chemical absorption of CO_2 with an alkaline metal carbonate as a solid sorbent. This is a modified hybrid technology of the adsorption and chemical absorption, which has an advantage with a simple and convenient operation for separation and recovery of CO_2 in flue gases. The development of sorbent, supporter, and regenerable scrubbing processes for CO_2 capture is the focus on the current study and is shown as follows:

Alkaline metal carbonate was supported on porous materials, such as an alumina gel (3), alumina (4), activated carbon (5–7), silica, and alumina vermiculite (8) to improve the sorption efficiency of the carbonate.

The carbonation reaction mechanism of alkaline metal carbonate by CO_2 under moist conditions to form alkali metal bicarbonate was verified by the x-ray diffraction method (5–7) and SEM image pattern of the solid surface (5–11). But the stoichiometric coefficient of H_2O in the carbonation reaction between the alkali metal carbonate, CO_2, and moisture depends on the type of carbonates (10) of anhydrate and hydrate and the kind of alkaline metal of Li, Na, K, Rb, Cs (5–11).

Most studies for CO_2 captured by the alkaline metal carbonate were carried out in a fixed-bed, but a thermogravimetric analyzer (12, 13) was used to get an initial rate of carbonation for the reaction kinetics of CO_2 sorption.

In mass transfer processes that accompany chemical reactions, the diffusion may have an effect on the reaction kinetics (14). The simplest and the most commonly used models (15–19) for a non-catalytic heterogeneous gas-solid reaction are the shrinking-core model and the homogeneous model with negligible pore diffusion limitations. Also the deactivation model (20–23) has been used to get the reaction kinetics using an analysis of reactivity of the solid reactant, which may be decreased by the change of the reaction circumstances. We believe that it is worthwhile to investigate to get the reaction kinetics of the gas-solid heterogeneous reaction such as the CO_2-carbonate reaction from comparison among theses models.

The objective of this study is to obtain the chemical kinetics of gas-solid reaction between CO_2, H_2O, and Na_2CO_3 using breakthrough data of CO_2 in a fixed bed, where the shrinking-core model, the homogeneous model, and the deactivation model are compared with one another, even if the carbonation mechanism of Na_2CO_3 by CO_2 and moisture (7) is very complicated.

THEORY

Anhydrous sodium carbonate(B) is reacted with CO_2(A) and moisture(W) to form sodium bicarbonate by the following equation (1):

$$Na_2CO_3(s) + CO_2(g) + H_2O(g) \longrightarrow 2NaHCO_3(s). \tag{1}$$

The reaction (1) is a non-catalytic heterogeneous gas-solid reaction. The mathematical analysis of this heterogeneous process must take into account the simultaneous influence of reaction and of heat and mass transfer to predict the conversion as a function of time for solid undergoing reaction. To obtain the chemical kinetics of the reaction (1) using CO_2 breakthrough data, three kinds of models such as the shrinking-core model and the homogeneous model, and the deactivation model are used as follows:

In the shrinking-core model (13) restricted to a nonporous solid with negligible pore diffusion limitations, the rate of movement of the sharp interface between the exhausted outer shell and the unreacted core of the solid can be related to the rate of reaction through a stoichiometric balance on Na_2CO_3:

$$-\frac{d}{dt}\left(\frac{4}{3}\pi r_c^3 \frac{\rho_B}{M_B}\right) = R_A \tag{2}$$

R_A is the rate of the chemical reaction, which occurs at the interface of the solid, is given as follows:

$$R_A = 4\pi r_c^2 k_1 C_A \tag{3}$$

where $k_1 = k_s C_w$ and constant if C_w is larger than C_A.

For this model, the relation between the conversion and the reaction time were expressed as

$$x_B = 1 - (1 - \frac{C_A k_1 M_B}{R\rho_B} t)^3 \tag{4}$$

x_B is defined as the reaction conversion of B as follows:

$$x_B = \frac{w_o - w}{w_o} = 1 - (\frac{r_c}{R})^3. \tag{5}$$

When the solid is porous and the rate of diffusion of the reactant gas is rapid, the gas will penetrate everywhere into the solid and the reaction will take place throughout the pellet. In some cases diffusional gradients may

exist inside the pellet, resulting in varying degrees of reaction within it. The homogeneous model (14) takes these effects into account and the reaction rate of B is given as follows:

$$-\frac{dC_B}{dt} = k_2 C_A C_B \tag{6}$$

where $k_2 = k_v C_w$.

For this model, the relation between the conversion and the reaction time were expressed as

$$x_B = 1 - \exp(-k_2 C_A t) \tag{7}$$

Breakthrough Analysis for the Shrinking-Core Model and the Homogeneous Model

In modeling fixed-bed non-catalytic reactors the continuity equation for the gas phase has to be coupled with the equation for the reaction of single particles. The problem is basically of a transient nature, since the rate of reaction decreases with time owing to the consumption of the solid reactant B. The major contributions in the modeling of fixed-bed non-catalytic systems have been made by researchers (15–17).

For an isothermal system the model equation for the reaction can be formulated as follows:

$$f_{bed}\frac{\partial C_A}{\partial t} - v\frac{\partial C_A}{\partial z} = r_v \tag{8}$$

where r_v is the rate of reaction of A per unit volume of the reactor. The rate can be related to the conversion of B by the following equation:

$$r_v = (1 - f_{bed})C_{Bo}\frac{dx_B}{dt} \tag{9}$$

where dx_B/dt is the rate of change of conversion of B for a pellet exposed to a bulk gas-phase concentration of C_A. The transient term $f_{bed}\partial C_A/\partial t$ is usually negligible (14) compared to other terms in Eq. (8); hence this equation can be expressed as

$$-v\frac{\partial C_A}{\partial z} = (1 - f_{bed})\frac{dx_B}{dt}. \tag{10}$$

Using Eq. (4) in the shrinking-core model, Eq. (10) is arranged as follows:

$$\frac{da}{dx} = -c_1\, a(1 - c_2\, a)^2 \tag{11}$$

where

$$a = \frac{C_A}{C_{Ao}}, \quad x = \frac{z}{Lz}, \quad c_1 = \frac{3k_1 w_f}{Q_g R \rho_B}, \quad c_2 = \frac{C_{Ao} k_1 M_B}{R\rho_B} t.$$

The initial condition in Eq. (11) is

$$a = 1 \text{ at } x = 0 \tag{12}$$

Eq. (11) is arranged for the whole range of the fixed bed as follows:

$$\int_a^1 \frac{da}{c_1 a(1 - c_2 a)^2} = 1 \tag{13}$$

Using Eq. (7) in the homogeneous model, Eq. (10) is arranged as follows:

$$\frac{da}{dx} = -c_3\, a \exp(-c_4\, a) \tag{14}$$

where

$$c_3 = \frac{k_2 w_f}{Q_g M_B}, \quad c_4 = k_2 C_{Ao} t.$$

Eq. (14) is arranged for the whole range of the fixed bed as follows:

$$\int_a^1 \frac{da}{c_3\, a \exp(-c_4\, a)} = 1. \tag{15}$$

The dimensionless concentration profiles with respect to the reaction time can be obtained by a combination of Simpson's rule and Runge-Kutta integrations for the shrinking-core model and the homogeneous model from Eqs. (11) and (14), respectively, and these concentration profiles are used to get the breakthrough data of CO_2 in the fixed bed.

Breakthrough Analysis for the Deactivation Model (18)

The formation of a dense product layer over the solid reactant creates an additional diffusion resistance and is expected to cause a drop in the reaction rate. One would also expect it to cause significant changes in the pore structure, the active surface area, and the activity per unit area of solid reactant with the reaction extent. All of these changes cause a decrease of activity of the solid reactant with time. In the deactivation model, the effects of all of these factors on the diminishing rate of CO_2 capture were combined in a deactivation rate term.

With assumptions of the pseudo-steady state and a constant concentration of water vapor, the isothermal species conservation equation for the reactant gas CO_2 in the fixed bed is

$$-Q_g \frac{dC_A}{dw} - k_o C_A \alpha = 0 \tag{16}$$

where $k_o = kC_w$.

In writing this equation, axial dispersion in the fixed bed and any mass transfer resistances were assumed to be negligible. According to the proposed deactivation model, the rate of change of the activity(α) of the solid reactant is expressed as

$$-\frac{d\alpha}{dt} = k_d C_A^n \alpha^m \tag{17}$$

where k_d is the deactivation rate constant. The zeroth solution of the deactivation models is obtained by taking $n = 0$. $m = 1$, and the initial activity of the solid as unity.

$$a = \exp[-\frac{k_o w}{Q_g}\exp(-k_d t)]. \tag{18}$$

This solution is equivalent to the breakthrough equation proposed by Suyadal et al. (21) and assumes a fluid phase concentration that is independent of deactivation processes along the reactor. More realistically, one would expect the deactivation rate to be concentration-dependent and, accordingly, the axial-position-dependent in the fixed bed.

To obtain the analytical solution of Eq. (16) and (17) by taking $n = m = 1$, an iterative procedure was applied. The procedure used here is similar to the procedure proposed by Dogu (22) for the approximate solution of nonlinear equations. In this procedure, the zeroth solution (Eq. (18)) is substituted into Eq. (17), and the first correction for the activity is obtained by the integration of this equation. Then, the corrected activity expression is substituted into Eq. (16), and the integration of this equation gives the first corrected solution for the breakthrough curve.

$$a = \exp\left[\frac{\left[1 - \exp\left(\frac{k_o w_f}{Q_g}(1 - \exp(-k_d t))\right)\right]}{1 - \exp(-k_d t)}\exp(-k_d t)\right]. \tag{19}$$

This iterative procedure can be repeated for further improvement of the solution. In this procedure, higher-order terms in the series solutions of the integrals are neglected. The breakthrough curve for the deactivation model with two parameters of k_o and k_d is calculated from the concentration profiles by Eq. (19).

EXPERIMENTAL

An Apparatus for CO_2 Capture and its Operation

In this study, sorption experiments (Fig. 1) were carried out in the presence of carbon dioxide and moisture with sodium carbonate sorbent in a fixed bed

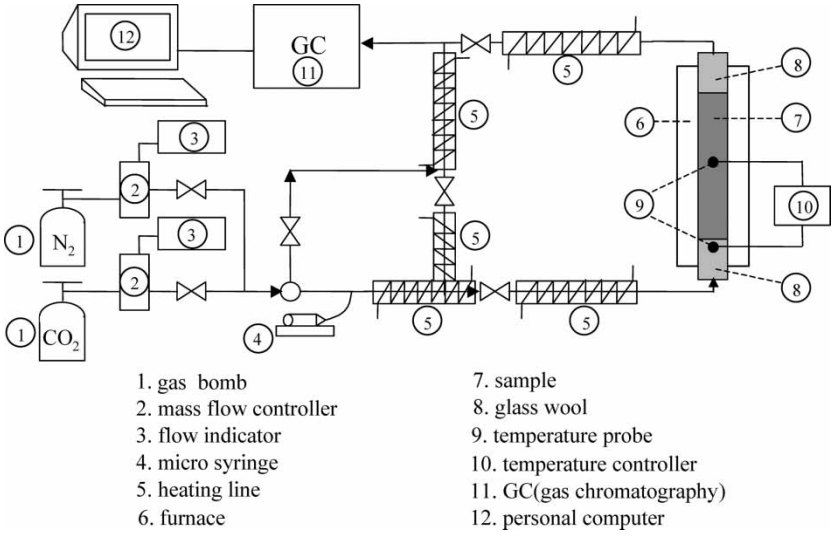

Figure 1. Schematic flow diagram of a fixed bed apparatus.

pyrex glass reactor (insider diameter = 2 cm). The water vapor was fed to the reactor through the line heated using a micro syringe. The flow rate of the gas mixture of carbon dioxide and nitrogen was in the range of 4–45 cm^3/min (measured at 25°C) and one atmospheric pressure, and the composition of CO_2 in the gas mixture was kept at 12% in most of the experiments. The flow rate of water was in the range of 0.1–2 cm^3/h. The amount of sorbent was in the range of 41–74 g. Experiments were repeated over a temperature range between 50($\pm$0.1) and 70($\pm$0.1)°C. A gas chromatography (detector; thermal conductivity detector, column; Haysep D(10 feet by 1/8 inch of stainless steel, detector temperature; 190($\pm$0.1)°C, feed temperature; 160($\pm$0.1)°C, flow rate of He; 25.7 cm^3/min. retention time of N_2, CO_2, H_2O; 0.9, 1.323, 20.6 min.) connected to the exit stream of the reactor allowed for an on-line analysis of CO_2, N_2, and water. The amount of gaseous mixture entering from the reactor to the automatic sampler of GC was 2 cm^3, and the oven temperature in GC was constant as 160($\pm$0.1)°C.

Sorbent particles were supported by glass wool from both sides. The reactor was placed into a tubular furnace equipped with a temperature controller. The length of the fixed sorbent section of the bed was in the range of 20–25 cm of the reactor according to the fed amount of NA_2CO_3. Temperature profiles were not observed within this section. The temperature probes were placed at two positions such as the middle position of the sample in the reactor and the inlet of the reactor. All of the flow lines between the reactor and the gas analyzer were heated to eliminate any condensation. Three-way valves placed before and after the reactor allowed for the flow of the gas mixture through the bypass line during flow rate adjustments.

The composition of the inlet stream was checked by the analysis of the stream flowing through the bypass line at the start of the experiments.

Physicochemical Properties of Sorbent

The size of the sorbent particle was measured using a sieve analyzer and its density was the value from its maker. The porosity of the fixed bed was measured by a conventional method using a mass cylinder. The values of d_p, ρ_B, and f_{bed} were 415.42 μm, 2315 kg/m^3 and 0.54, respectively.

RESULTS AND DISCUSSION

Comparison of the Proposed Models

To ensure the condition of the concentration of water vapor to be constant for the analysis of three proposed models, the concentrations of CO_2 and water vapor at inlet of the fixed bed were measured at the experimental conditions mentioned below, and their values were 2.4 and 78.5%, respectively. Because the concentration of water vapor is much larger than that of CO_2, the concentration of water vapor can be assumed to be constant.

To test the agreement of the data with the proposed models such as the shrinking-core, and the homogeneous and the deactivation model, the concentrations of CO_2 at the exit of the fixed bed were measured according to the change of the reaction time under the typical experimental conditions such as the flow rate of the gaseous mixture with CO_2 and N_2; 10 cm^3/min, the composition of CO_2 in the gaseous mixture; 12%(moisture free), flow rate of water; 1.49 cm^3/h, weight of sorbent; 56 g, and sorption temperature; 60°C, from which the breakthrough data of CO_2 were obtained and plotted as circles in Fig. 2. As shown in Fig. 2, the concentration of CO_2 was increased as increase of the reaction time.

The breakthrough curve and the reaction rate constant (k_1) in the shrinking-core model were estimated by the following procedure: the concentration profile of CO_2 is obtained from the numerical solution of Eq. (11) with the initial condition of Eq. (12) using the fourth order Runge-Kutta method at a given reaction time, and then, k_1 is adjusted in order that the integration value of the left side of Eq. (13) using Simpson's rule may be equal to 1. The adjusted k_1 was 2.26×10^{-4} m/min and the breakthrough curve was obtained from the concentration profile with respect to the reaction time and drawn as a short-dash line in Fig. 2.

The procedure to get the breakthrough curve and the reaction rate constant(k_2) in the homogeneous model is the same as that in the shrinking-core model except for Eq. (14) and (15). The adjusted k_2 was 0.147 m^3/kmol·min, and drawn as a dash-dot line in Fig. 2. As shown in

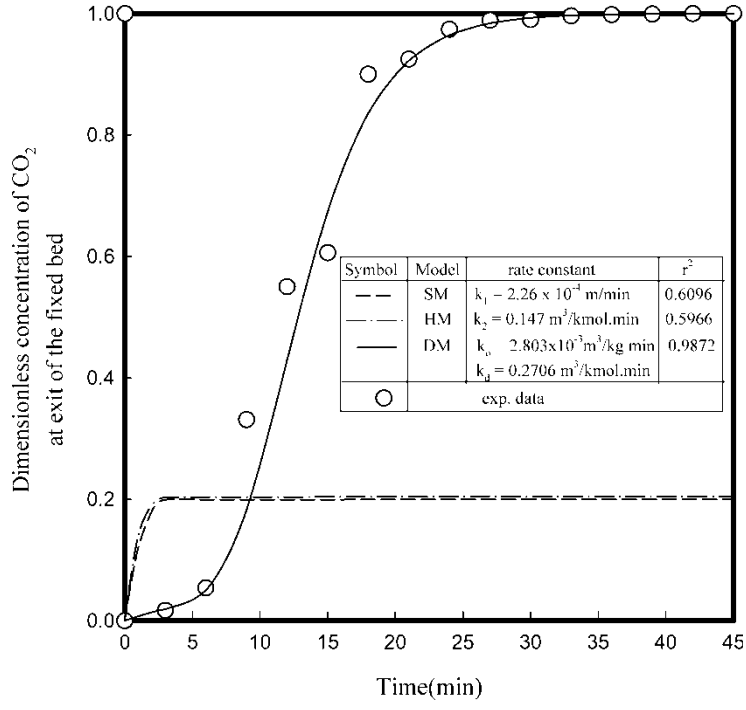

Figure 2. Breakthrough curves of CO_2 in the fixed bed. ($Q_g = 10\ cm^3/min$, $Q_w = 1.49\ cm^3/min$, $y_A^* = 0.12$, $W_f = 56$ g; SM = Shrinking-core model, HM = Homogeneous model, DM = Deactivation model.)

Fig. 2, the calculated breakthrough curves of CO_2 for two models did not agree with the breakthrough data in the whole range of the stream time. It may be said that both the models are not the proper models for the sorption kinetics of CO_2 on Na_2CO_3.

On other hand, the breakthrough curve from Eq. (19) in the deactivation model was evaluated by analysis of the experimental breakthrough data using a nonlinear least squares technique with two parameters of k_o of $2.803 \times 10^{-3}\ m^3/kg \cdot min$ and k_d of $0.2706\ m^3/kmol \cdot min$, and drawn as a solid line in Fig. 2. As shown in Fig. 2, the regression analysis of the experimental breakthrough data presented a very good agreement with the breakthrough equation Eq. (19) with regression coefficient of 0.987.

Figure 3 shows a TGA thermogram of anhydrous Na_2CO_3, anhydrous $NaHCO_3$, and a product formed during the reaction time of 45 minutes. As shown in Fig. 3, there is no weight change in Na_2CO_3, a 36.4% weight loss in $NaHCO_3$, and a 3.2% weight loss in the product.

Figure 4(a) shows the surface pattern by SEM of anhydrous Na_2CO_3, the reactant for all of the experimental run. A uniform pore structure of a small

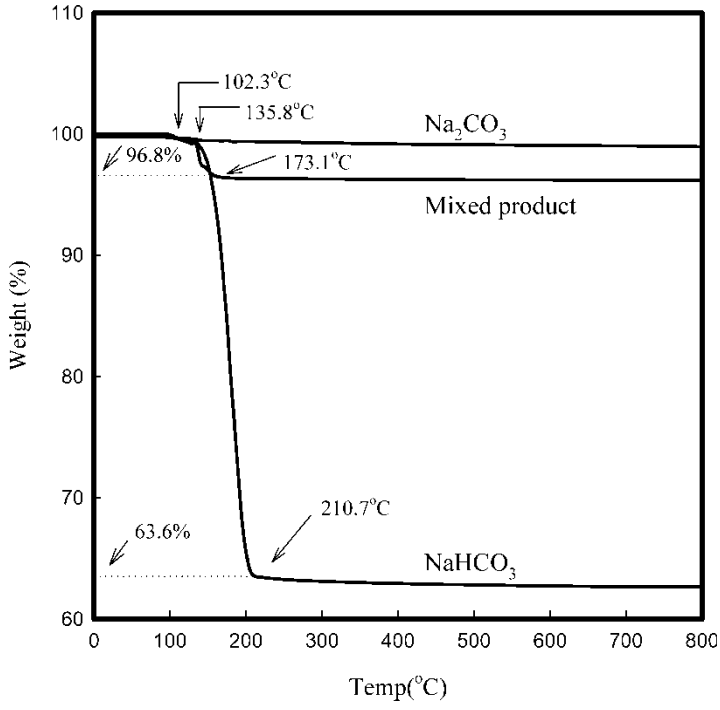

Figure 3. TGA thermogram of Na_2CO_3, $NaHCO_3$ and product of the carbonation of Na_2CO_3.

size is observable in the material. Figure 4(b) shows anhydrous $NaHCO_3$. The surface pattern is very different from that of the reactant. Fig. 4 (c) illustrates a product in which some $NaHCO_3$ was formed during the reaction time of 45 minutes. It may be said that the product was formed of Na_2CO_3 and $NaHCO_3$.

It may be concluded that the deactivation model with two parameters can be used to analyze the breakthrough data of CO_2 in the fixed bed, because changes in the pore structure causes significant variations on the carbonation rates and the reactivity of the reactant from the results of Figs. 3 and 4. The deactivation model was more useful rather than the shrinking-core model and the homogeneous model to explain the chemical mechanism of gas-solid non-catalytic reactions as that in the paper about the kinetics of char gasification of lignites with CO_2 using the thermogravimetric analyzer of Yasyerli, et al. (23).

Kinetics of CO_2 Sorption on Na_2CO_3

To investigate the sorption kinetics of CO_2 on Na_2CO_3 using a two–parameter deactivation model, the breakthrough curves of CO_2 were measured according

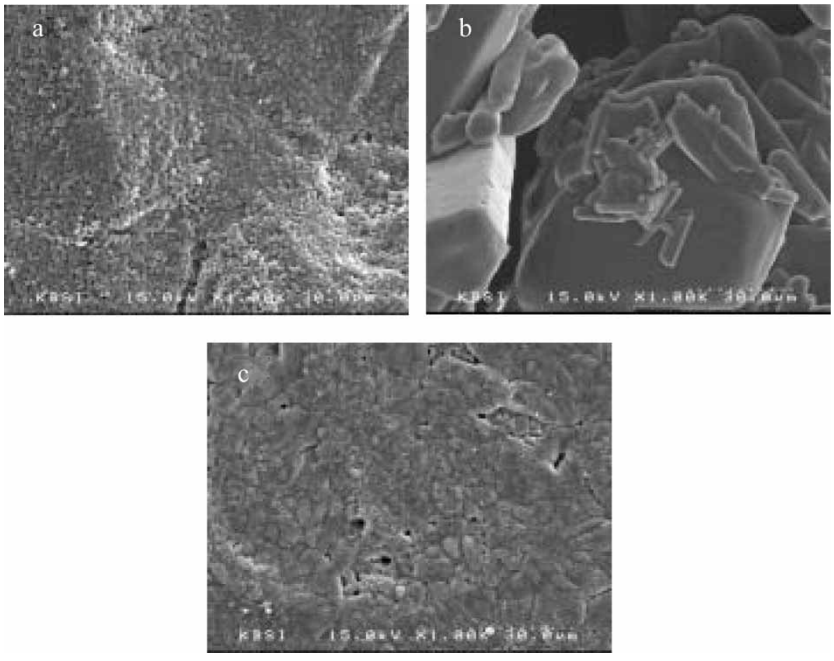

Figure 4. SEM image patters of the surface of solid. (a: Na_2CO_3, b: $NaHCO_3$, c: product of the carbonation of Na_2CO_3).

to the changes of the experimental variables such as the gaseous flow rate of CO_2 and N_2, the flow rate of water, the weight of sorbent, and the sorption temperature.

Effect of Flow Rate of Gaseous Mixture of CO_2 and N_2

To investigate the effect of the flow rate of gaseous mixtures of CO_2 and N_2 on the kinetics, the breakthrough curves of CO_2 were measured in the range of the gaseous flow rate of CO_2 and N_2 of $4-20\ cm^3/min$ before adding water at a fixed mole fraction of CO_2 of 0.12 in the gaseous mixtures, various flow rates of water, and 60°C. The gaseous mixtures at the inlet of the column consist of three components such as CO_2, N_2, and water vapor, and the concentrations of CO_2 and water vapor depend on the flow rate of gaseous mixtures of CO_2 and N_2 and the flow rate of water. Because the concentration of water vapor at the inlet of the fixed bed should have the same condition as one another for the various changes of the flow rate of gaseous mixtures of CO_2 and N_2, the flow rates of water fed into the micro syringe were controlled using the mass balance for three components. The measured values of breakthrough curves of CO_2 were plotted against the reaction time with parameters of the flow rate of gaseous mixtures of CO_2 and N_2 and

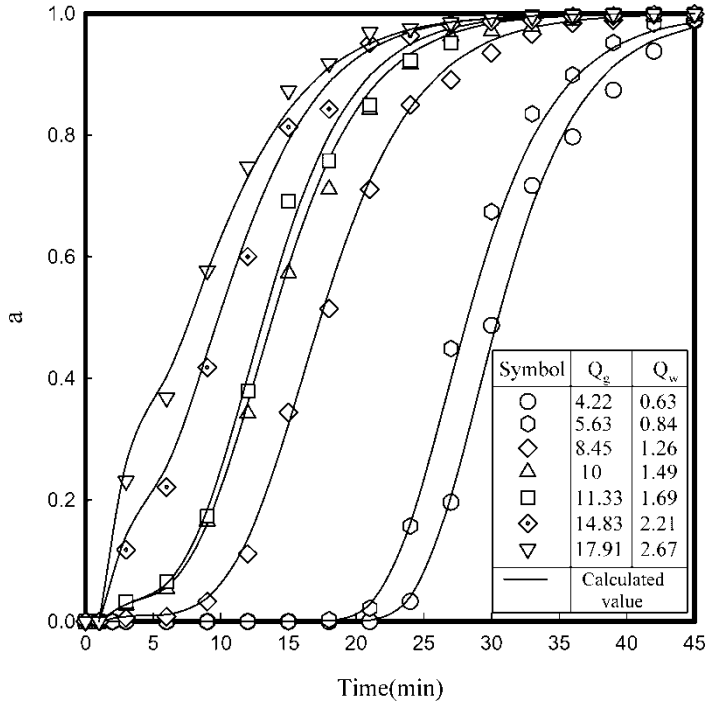

Figure 5. Effect of the flow rate of mixture of N_2 and CO_2 on the breakthrough curves of CO_2 at 60°C. ($W_f = 56$ g).

that of water as various symbols in Fig. 5. As shown in Fig. 5, a shift of breakthrough curves to smaller times was observed at more flow rate of the gaseous mixture with a decrease in sorption capacity. This means that the reaction conversion decreases as the space time of the gaseous mixtures in the fixed bed, i.e., the reaction time decreases. Analysis of the experimental breakthrough data using a nonlinear least squares technique was in good agreement with Eq. (19). The evaluated values of k obtained by k_o and C_w, and k_d are reported in Table 1, and calculated curves using Eq. (19) are shown in Fig. 5 as solid lines with regression coefficient more than 0.997. As shown in Table 1, the values of k and k_d are almost the same as one another.

Effect of Flow Rate of Water

To know the effect of the flow rate of water on the kinetics, the breakthrough curves of CO_2 were measured in the range of the flow rate of water of 1-2 cm^3/h at given concentrations of CO_2 in a gaseous mixture of CO_2 and N_2, and 60°C. The flow rate and CO_2 concentration of gaseous mixtures of CO_2 and N_2 were adjusted according to the change of the flow rate of water

Table 1. Rate parameters for various experimental conditions at 60°C

Q_g (cm^3/min)	Q_w (cm^3/h)	w_f (g)	$y_A{}^*$ (−)	c_w (M)	k_o x 10^3 (m^3/kg · min)	k (m^6/ kmol · kg · min)	k_d (1/min)	r^2 (correlation)
4.22	0.63	56	0.12	0.0282	2.544	0.0902	0.2384	0.998
5.63	0.84	56	0.12	0.0282	3.037	0.1077	0.2316	0.998
8.45	1.26	56	0.12	0.0282	2.617	0.0928	0.2204	0.999
10.0	1.49	56	0.12	0.0282	2.648	0.0939	0.2363	0.998
11.33	1.69	56	0.12	0.0282	3.006	0.1066	0.2483	0.997
14.83	2.21	56	0.12	0.0282	2.806	0.0995	0.2304	0.997
17.91	2.67	56	0.12	0.0282	2.611	0.0926	0.2116	0.997
21.09	1.0	56	0.057	0.0190	1.870	0.0984	0.2592	0.998
16.57	1.2	56	0.072	0.0227	2.254	0.0993	0.2284	0.996
7.51	1.6	56	0.16	0.0303	2.951	0.0974	0.2411	0.999
10.0	1.49	41	0.12	0.0282	2.800	0.0993	0.2706	0.996
10.0	1.49	74	0.12	0.0282	2.950	0.1046	0.2158	0.997

in order that the concentration of CO_2 at the inlet of the column may be the same as mentioned above. The measured values of breakthrough curves of CO_2 were plotted against the reaction time with parameters of the flow rate and CO_2 concentration of gaseous mixtures of CO_2 and N_2 as various symbols in Fig. 6. As shown in Fig. 6, the sorption capacity of CO_2 increases at more flow rate of water. This means that the reaction conversion increases as the concentration of reactant(water) increases. The values of k and k_d are evaluated along the same procedure mentioned above and listed in Table 1. The calculated curves using Eq. (19) are shown in Fig. 6 as solid lines with regression coefficient more than 0.998. As shown in Table 1, the values of k and k_d are almost the same one another.

Effect of Amount of Na_2CO_3

To observe the effect of the sorbent amount on the kinetics, the breakthrough curves of CO_2 were measured in the range of the mass of Na_2CO_3 of 0.041–0.074 kg at flow rate and concentration of CO_2 in a gaseous mixture of CO_2 and N_2 of 10 cm^3/min and 0.12 mole fraction, and the flow rate of the

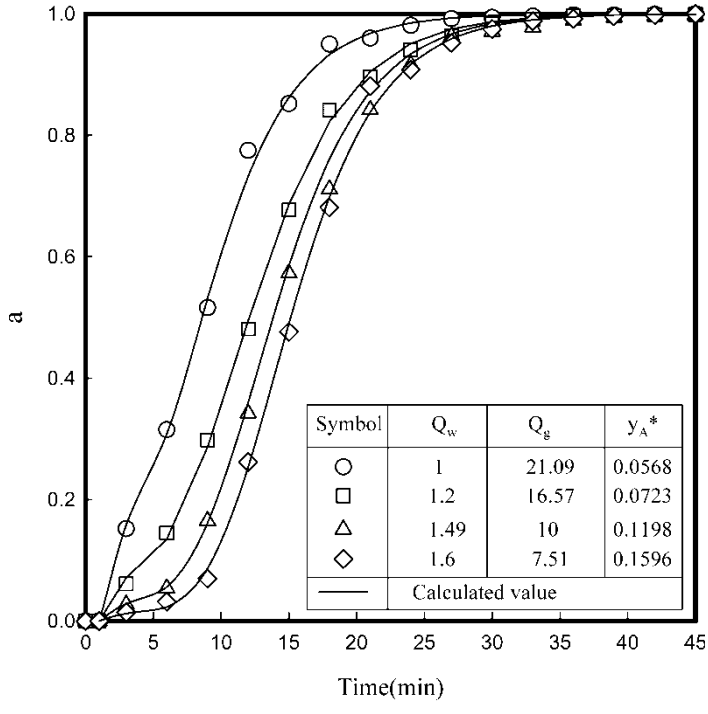

Figure 6. Effect of the flow rate of water on the breakthrough curves of CO_2 at 60°C. ($W_f = 56$ g).

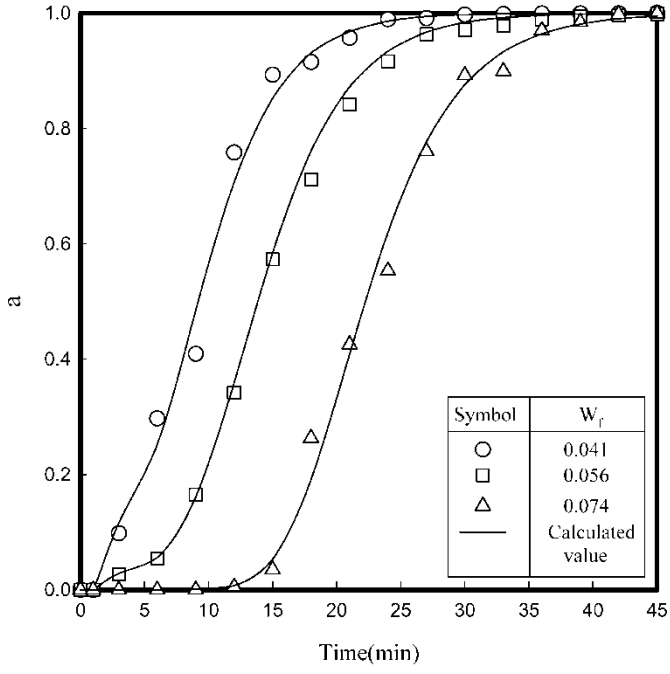

Figure 7. Effect of the flow rate of amount of Na_2CO_3 on the breakthrough curves of CO_2 at 60°C. ($Q_g = 10\ cm^3/min$, $Q_w = 1.49\ cm^3/h$).

water was 1.49 cm^3/h, and 60°C. The measured values of breakthrough curves of CO_2 were plotted against the reaction time with parameters of the amount of water as various symbols in Fig. 7. As shown in Fig. 7, the sorption capacity of CO_2 increases when more sorbent is added. This means that the reaction conversion increases as the concentration of the reactant (sorbent) increases. The evaluated values of k and k_d are reported in Table 1, and calculated curves using Eq. (19) are shown in Fig. 7 as solid lines with regression coefficient more than 0.996. As shown in Table 1, the values of k and k_d are almost the same as one another.

Effect of Reaction Temperature

To find the dependence of the reaction parameters on the sorption temperature, the breakthrough curves of CO_2 were measured in the temperature range between 50 and 70°C at flow rate and concentration of CO_2 in a gaseous mixture of CO_2 and N_2 of 10 cm^3/min and 0.12 mole fraction, the flow rate of water 1.49 cm^3/h, and sorbent of 56 g. The values of k_o and k_d were evaluated from the analysis of the experimental breakthrough data using a nonlinear least squares technique along the same procedure mentioned

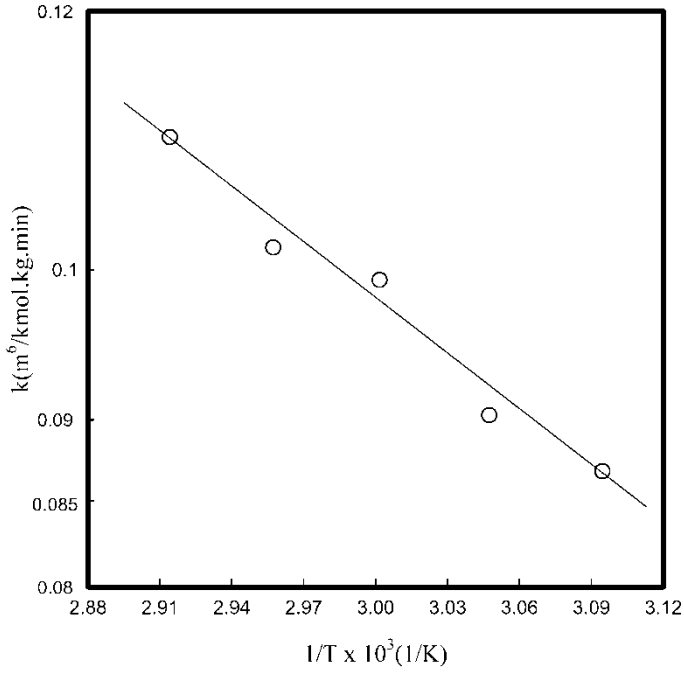

Figure 8. Arrhenius plot of reaction rate constant. ($Q_g = 10$ cm^3/min, $Q_w = 1.49$ cm^3/h, $y_A{}^* = 0.12$, $W_f = 56$ g)

above, and k was obtained using k_o and the initial concentration of moisture. The Arrhenius plots are shown in Figs. 8 and 9, respectively. As shown in these two figures, the plots satisfy the linear relationship. Using the values of the slope and the intercept of these straight lines, the empirical equations are obtained as follows:

$$k = 4.853 \exp\left(-\frac{2.856}{RT}\right) \tag{20}$$

$$k_d = 28.751 \exp\left(-\frac{3.092}{RT}\right) \tag{21}$$

CONCLUSIONS

The breakthrough data of CO_2 were measured in a fixed bed to observe the reaction kinetics of CO_2 sorption among sodium carbonate, carbon dioxide, and moisture under the experimental conditions such as the flow rate of gaseous mixture of 4–20 cm^3/min, the flow rate of water of 1–2 cm^3/h, mass of sodium carbonate of 0.041–0.074 kg, and reaction temperature of

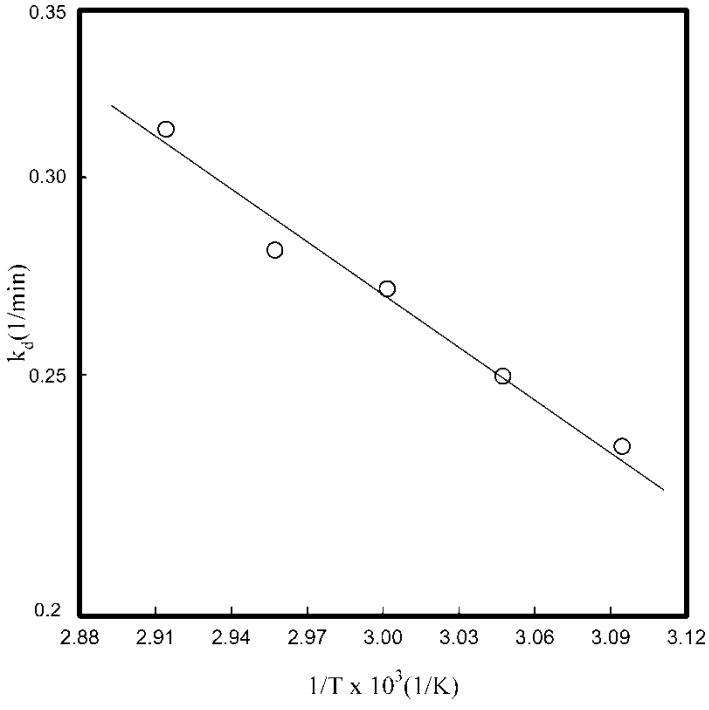

Figure 9. Arrhenius plot of deactivation rate constant. ($Q_g = 10\ cm^3/min$, $Q_w = 1.49\ cm^3/h$, $y_A^* = 0.12$, $W_f = 56\ g$)

50–70°C. Good agreement of the deactivation model was obtained with the experimental breakthrough data in the heterogeneous solid-gas reaction system with changes in the pore structure and the reactivity of the solid reactant. The sorption rate constant and the deactivation rate constant were evaluated by analysis of the experimental breakthrough data using a nonlinear least squares technique and described as the Arrhenius form.

NOMENCLATURE

C_A	concentration of A in bulk phase(kmol/m^3)
C_w	initial concentration of water vapor(kmol/m^3)
C_B	concentration of solid B in bulk phase(kmol/m^3)
d_p	diameter of solid B(m)
f_{bed}	bed voidage
k	initial second-order sorption rate constant(m^6/kmol · kg · min)
k_o	initial sorption rate constant(m^3/kg · min)
k_1	first-order reaction rate constant(m^4/kmol · min)
k_2	second-order reaction rate constant(m^3/kmol · min)

k_d	deactivation rate constant at n = 0(1/min), or n = 1 (m^3/kmol · min)
k_v	reaction rate constant in homogeneous model(m^6/$kmol^2$ · min)
Lz	length of the reaction section(m)
M_B	molecular weight of reactant B(kg/kmol)
r	radius axis of spherical coordinate(m)
r_v	reaction rate of A per unit volume of the fixed bed(kmol/m^3 · min)
R	radius of reactant B(m)
R_A	mass transfer rate of species A(kmol/min)
Q_g	volumetric flow rate of gaseous mixture(m^3/min)
Q_w	volumetric flow rate of water(m^3/hr)
t	reaction time(min)
T	reaction temperature(K)
v	superficial velocity of gaseous mixtures(m/min)
x_B	reaction conversion of solid B
W_f	weight of solid B(kg)
y_A	mole fraction of A
y_A^*	mole fraction of A with moisture free
z	axial coordinate in fixed bed(m)

Greek Letters

α	activity of sodium carbonate
ρ_B	density of reactant B (kg/m^3)

Subscripts

A	CO_2
B	Na_2CO_3
o	initial value
w	moisture

ACKNOWLEDGMENTS

This research was supported by a grant(DA1-202) from Carbon Dioxide Reduction & Sequestration Research Center, one of twenty-first century's frontier programs founded by the Ministry of Science and Technology of the Korean Government.

REFERENCES

1. Aresta, M. (2003) *Carbon Dioxide Recovery and Utilization*; Kluwer Academic Pub.: Boston, p. 53.
2. Bartoo, R.K. (1984) Removing acid gas by the benfield process. *Chem. Eng. Prog.*, 80: 35–39.

3. Fuchs, W., Syosett, N.T. (1970) Method of removing carbon dioxide and water from air. U. S. Patent 3,511,595 May 12.
4. Gidaspow, D. and Onischak, M (Feb. 11, 1975) Process for regenerative sorption of CO_2. U. S. Patent 3,865,924.
5. Hirano, S., Shigomoto, N., Yamada, S., and Hayashi, H. (1995) Cyclic fixed-bed operations over K_2CO_3-oncarbon for the recovery of carbon dioxide under moist conditions. *Bull. Chem. Soc. Jpn.*, 68: 1030–1035.
6. Hayashi, H., Taniuchi, H.J., Furuyashiki, N., Sugiyama, S., Hirano, S., Shigemoto, N., and Nonaka, T. (1998) Efficient recovery of carbon dioxide from flue gases of coal-fired power plants by cyclic fixed-bed operations over K_2CO_3-on-carbon. *Ind. Eng. Chem. Res.*, 37: 185–194.
7. Shigemoto, T., Sugiyama, S., and Hayashi, H. (2005) Bench-scale CO_2 recovery from moist flue gases by various alkali carbonates supported on activated carbon. *J. Chem. Eng. Jpn*, 38: 711–717.
8. Okunev, A.G., Sharnov, V.E., Aristov, Y.I., and Parmon, V.N. (2004) Sorption of carbon dioxide from wet gases by K_2CO_3-in- porous matrix: Influence of the matrix nature. *React. Kinet. Catal. Lett.*, 71: 355–362.
9. Ball, M.C., Strachan, A.N., and Strachan, R.M. (1991) Thermal decomposition of solid Wegschiderite, Na_2CO_3-$3NaHCO_3$. *J. Chem. Faraday, Trans.*, 87: 1911–1914.
10. Ball, M.C., Clarke, R.A., and Strachan, A.N. (1991) Investigation of the formation of Wegschiderite, Na_2CO_3-$3NaHCO_3$. *J. Chem. Faraday, Trans.*, 87: 3683–3686.
11. Ball, M.C., Snelling, C.M., Strachan, A.N., and Strachan, R.M. (1992) Thermal decomposition of solid sodium sesquicarbonate, Na_2CO_3-$NaHCO_3$-$2H_2O$. *J. Chem. Faraday, Trans.*, 88: 631–636.
12. Hoffman, J.S. and Pennline, H.W. (2001) Study of regenerable sorbents for CO_2 capture. *J. Energy & Environ. Res.*, 1: 90–100.
13. Green, D.A., Turk, B.S., Gupta, R.P., McMichael, W.J., Harrison, D.P., and Liang, Y. (Jan. 2003) Carbon dioxide capture from flue gas using dry regenerable sorbents. In *Quarterly Technical Progress Report*. Louisiana State University.
14. Doraiswamy, L.K. and Sharma, M.M. (1984) *Heterogeneous Reactions*; John Wiley & Sons, Inc.: New York; Vol. 1.
15. Ishida, M. and Wen, C.Y. (1968) Comparison of kinetics and diffusional models for solid-gas reactions. *AIChE J.*, 14: 311–317.
16. Ramachandran, P.A. and Kulkarni, B.D. (1980) Approximate analytical solution to gas-solid noncatalytic reaction problem. *Ind. Eng. Chem. Res. Process Design Dev.*, 19: 717–719.
17. Evans, J.W. and Song, S. (1974) Application of a porous pellet model to fixed, moving, and fluidized bed gas-solid reactors. *Ind. Eng. Chem. Process Des. Develop.*, 13: 146–152.
18. Sampath, B.S., Ramachandran, P.A., and Hughes, R. (1975) Modeling of non-catalytic gas-solid reactors-II. Transient simulation of a packed bed reactor. *Chem. Eng. Sci.*, 30: 135–143.
19. Ranade, M.G. and Evans, J.W. (1980) The reaction between a gas and a solid in a nonisothermal packed bed: Simulation and experiments. *Ind. Eng. Chem. Process Des. Develop.*, 19: 118–123.
20. Yasyerli, S., Dogu, G., and Ar, I. (2001) Activities of copper oxide and Cu-V and Cu-Mo mixed oxides for H_2S removal in the presence and absence of hydrogen and predictions of a deactivation model. *Ind. Eng. Chem. Res.*, 40: 5206–5214.

21. Suyadal, Y., Erol, M., and Oguz, M. (2000) Deactivation model for the absorption of trichloroethylene vapor on an activated carbon. *Ind. Eng. Chem. Res.*, 39: 724–730.
22. Dogu, T. (1986) Extension of moment analysis to nonlinear systems. *AIChE J.*, 32: 849–852.
23. Yasyerli, S., Dogu, T., Dogu, G., and Ar, I. (1996) Deaction model for textural effects on kinetics of gas-solid no-catalytic reactions char gasification with CO_2. *Chem. Eng. Sci.*, 51: 2523–2528.